I R A M P
12(1), Jan 2021, pp. 9-16

ISSN: 2229-39-44

A Principle for Spectroscopic Diagnostics of Weak Electrostatic Waves in Magnetized Plasmas

E. OKS[1], E. DALIMIER[2] AND P. ANGELO[2]

[1]*Physics Department, 380 Duncan Drive, Auburn University, Auburn, AL 36849, USA*
[2]*LULI - Sorbonne Université ; CNRS, Ecole Polytechnique, CEA: Université Paris-Saclay – F-75252 Paris cedex 05, France*
Corresponding author: goks@physics.auburn.edu

ABSTRACT: There are various methods for spectroscopic diagnostics of electrostatic waves in plasmas for the range of the field strength from about 1 kV/cm to about 5 GV/cm. In the present paper we extend this range down to about 10 V/cm or even lower. We use the fact that for relatively strong magnetic fields, hydrogen atoms can have delocalized bound states of almost macroscopic dimensions. Therefore, such states are characterized by a Giant Electric Dipole Moment (GEDM), thus making them very sensitive to an external electric field. We consider the manifestations of the GEDM states in hydrogen spectral line profiles in the presence of a quasimonochromatic electrostatic wave of a frequency ω in a plasma. We demonstrate that in this situation, hydrogen spectral lines can exhibit quasi-satellites, which are the envelopes of Blochinzew-type satellites. We show that the *distinctive feature* of such quasi-satellites is that their peak intensity is located at the same distance from the line center (in the frequency scale) for all hydrogen spectral lines, the distance being significantly greater than the wave frequency ω. At the absence of the GEDM (and for relatively strong electrostatic waves), the maxima of the satellite envelopes would be at different distances from the line center for different hydrogen lines.

Keywords: strong magnetic fields, center-of-mass effects, giant electric dipole moments, supersensitive diagnostics of electrostatic waves in plasmas

1. INTRODUCTION

There are various methods for spectroscopic diagnostics of electrostatic waves in plasmas for the range of the field strength from about 1 kV/cm to about 5 GV/cm – see, e.g., books [1, 2]. These methods employ the shape of spectral lines of different atoms and ions. In the present paper we offer a way for extending the sensitivity of such methods to ~ 10 V/cm or even lower, as follows.

There is plenty of studies showing that for hydrogenic atoms/ions in a uniform magnetic field, the center-of-mass motion and the relative (internal) motion are coupled by the magnetic field and, rigorously speaking, cannot be separated – see, e.g., papers [3-5] and references therein. A pseudoseparation is possible for hydrogen atoms. It leads to a Hamiltonian for the relative motion that depends on a center-of-mass integral of the motion **K** called pseudomomentum, but does not depend on the center of mass coordinate [5]. We remind that the pseudomomentum **K** is the canonical variable conjugated to the center of mass coordinate.

A diamagnetic potential term in the Hamiltonian for the relative motion is responsible for the formation of an additional potential well –far away from the hydrogen nucleus (proton). For relatively strong magnetic fields, the new bound states inside this well are delocalized states of almost macroscopic dimensions. Therefore, the bound state inside this well is characterized by a Giant Electric Dipole Moment (GEDM), thus making such states very sensitive to an external electric field.

In the present paper we consider the effect of a quasimonochromatic electrostatic wave of a frequency ω in a plasma on hydrogen spectral lines at the presence of the GEDM states. We show that in this situation, hydrogen spectral lines can exhibit quasi-satellites. The quasi-satellites are envelopes of Blochinzew-type satellites [6], the latter being separated from the line center by multiples of the wave frequency ω (in the frequency scale) in both the red and blue wings. We demonstrate that the distinctive feature of such quasi-satellites (at the presence of the GEDM states) is that their peak intensity is located at the same distance from the line center (in the frequency scale) for all hydrogen spectral lines, the distance being significantly greater than the wave frequency ω. We show that this effect would allow measuring the amplitude of electrostatic waves in plasmas down to ~ 10 V/cm or even lower. We provide an example for the conditions of edge plasmas of tokamaks.

2. DETAILS OF THE EFFECT

In the Hamiltonian of the relative (internal) motion for the hydrogen atom in a magnetic field **B**, the potential energy has the form (see, e.g., Schmelcher-Cederbaum paper [7], Eq. (6))

$$V = [e^2/(2Mc^2)]\mathbf{B}x\mathbf{r} - [|e|/(Mc](\mathbf{B}x\mathbf{K})\mathbf{r} - e^2/r, \tag{1}$$

where **K** is the pseudomomentum, M is the mass of the hydrogen atom, c is the speed of light, and e is the electron charge. We follow paper [7] in choosing $e < 0$; we also note that in paper [7] it was set $c = 1$. In Eq. (1), $(\mathbf{B}x\mathbf{K})\mathbf{r}$ stands for the scalar product (also known as the dot-product) of vector **r** and vector $(\mathbf{B}x\mathbf{K})$.

We also assume the same configuration as chosen in paper [7]: $\mathbf{B} = (0, 0, B)$, $\mathbf{K} = (0, K, 0)$, where $K > 0$. Then Eq. (1) takes the form:

$$V = [e^2B^2/(2Mc^2)](x^2 + y^2) + [|e|BK/(Mc]x - e^2/(x^2 + y^2 + z^2)^{1/2}. \tag{2}$$

For simplifying equations, we introduce the following scaled potential energy V_s:

$$V_s = Mc^2V/(e^2B^2). \tag{3}$$

Then Eq. (2) can be rewritten as follows:

$$V_s = (x^2 + y^2)/2 + [Kc/(|e|B)]x - Mc^2/[B^2(x^2 + y^2 + z^2)^{1/2}]. \tag{4}$$

By equating partial derivatives of V_s with respect to y and z to zeros, we find that this occurs at $y = z = 0$ (as in paper [7]). The partial derivative of V_s with respect to x that we calculate for finding extrema of the potential, has the form:

$$\partial V_s/\partial x = x + Kc/(|e|B) + Mc^2x/[B^2(x^2 + y^2 + z^2)^{3/2}]. \tag{5}$$

At $y = z = 0$, Eq. (5) becomes:

$$\partial V_s/\partial x = x + Kc/(|e|B) + (Mc^2/B^2)\,(\text{sign } x)/x^2. \tag{6}$$

We remind that sign $x = 1$ for $x > 0$ or sign $x = -1$ for $x < 0$.

On equating $\partial V_s/\partial x$ from Eq. (6) to zero, we arrive to the following equation:

$$x^3 + [Kc/(|e|B)]x^2 + (Mc^2/B^2)(\text{sign } x) = 0. \tag{7}$$

Thus, for $x > 0$ and for $x < 0$, Eq. (7) leads to two different equations.

For $x > 0$, Eq. (7) becomes:

$$x^3 + [Kc/(|e|B)]x^2 + (Mc^2/B^2) = 0. \tag{8}$$

Obviously, Eq. (8) does not have positive roots.

For $x < 0$, Eq. (7) leads to

$$|x|^3 - [Kc/(|e|B)]|x|^2 + (Mc^2/B^2) = 0. \tag{9}$$

Equation (9) is equivalent to Eq. (8b) from paper [7]; we remind that in paper [7] it was set c = 1 and e = –1.

The polynomial in Eq. (9) has either two or zero real roots. Thus, the total number of roots of Eq. (7) is also either two or zero – since there are no positive roots.

We note in passing that the authors of paper [7] erroneously stated that $\partial V_s/\partial x$, calculated at y = z = 0, can have three real roots. Their error originates from the fact that they missed the factor (sign x) in the corresponding equation.

We introduce the scaled magnetic field b and the scaled pseudomomentum k, as follows

$$b = B/(cM^{1/2}) , \qquad k = K/(|e|M^{1/2}), \tag{10}$$

where b has the dimension of $cm^{-3/2}$ and k has the dimension of $cm^{-1/2}$. Below, while using particular numerical values of b and k, we omit the dimensions for brevity.

With these notations, Eq. (9) simplifies as follows:

$$|x|^3 - (k/b)|x|^2 + 1/b^2 = 0. \tag{11}$$

The discriminant Δ of this cubic equation is

$$\Delta = (4k^3 - 27b)/b^5. \tag{12}$$

So, Eq. (11) has two distinct real negative roots if Δ > 0, i.e. if

$$k > 3(b/4)^{1/3}. \tag{13}$$

The exact analytical results for the two real roots x_1 and x_2 of Eq. (11) are as follows:

$$x_1 = -k/(3b) - (1 + 3^{1/2}i)\, k^2/\{2^{2/3}3b[27b - 2k^3 + 3^{3/2}(27b^2 - 4k^3b)^{1/2}\,]^{1/3}\} - (1 - 3^{1/2}i)\,[27b - 2k^3 + 3^{3/2}(27b^2 - 4k^3b)^{1/2}\,]^{1/3}/(2^{1/3}6b). \tag{14}$$

$$x_2 = -k/(3b) - (1 - 3^{1/2}i)\, k^2/\{2^{2/3}3b[27b - 2k^3 + 3^{3/2}(27b^2 - 4k^3b)^{1/2}\,]^{1/3}\} - (1 + 3^{1/2}i)\,[27b - 2k^3 + 3^{3/2}(27b^2 - 4k^3b)^{1/2}\,]^{1/3}/(2^{1/3}6b). \tag{15}$$

It should be emphasized that, despite the presence of the imaginary unit i in Eqs. (14) and (15), they yield real numbers for x_1 and x_2 under the condition (13).

Figure 1 shows the plot of the root x_1 (solid line) and x_2 (dashed line) versus the scaled magnetic field b for the scaled pseudomomentum k = 10 (corresponding to K = 0.031 a.u. = 6.2×10^{-21} g cm/s). It is seen that the largest (by the absolute value) root is x_1.

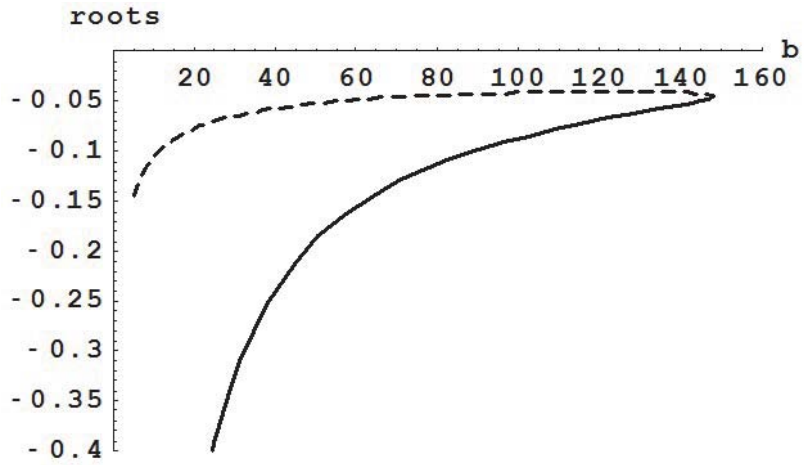

Fig. 1. Plot of the root x_1 (solid line) and x_2 (dashed line) of Eq. (11) versus the scaled magnetic field b for the scaled pseudomomentum k = 10. The vertical scale is in cm.

It is easy to find out that at $x = x_1$ one has $\partial^2 V_s/\partial x^2 > 0$, so that the scaled potential energy V_s has a minimum at $x = x_1$ (under condition (13)). At $x = x_2$ one has $\partial^2 V_s/\partial x^2 < 0$, so that the scaled potential energy V_s has a maximum at $x = x_2$ (under condition (13)).

The scaled potential energy V_s at y = z = 0 has the form:

$$V_s = x^2/2 + kx/b - 1/(b^2|x|). \tag{16}$$

Figure 2 shows the plot of the scaled potential energy V_s from Eq. (16) versus the coordinate x (in cm) at the scaled magnetic field $b = 1.3 \times 10^6$ (corresponding to B = 5 Tesla) for the following three values of the scaled pseudomomentum: k = 400 corresponding to K = 1.25 a.u. (solid line), k = 206 corresponding to K = 0.64 a.u. (dashed line), k = 100 corresponding to K = 0.31 a.u. (dotted line). These three values of k correspond to the values of the discriminant in Eq. (12) $\Delta > 0$, $\Delta = 0$, and $\Delta < 0$, respectively. It is seen that for k = 400, the plot shows a maximum and minimum at $x < 0$; for k = 206, the plot exhibits a flat part caused by the merging of the maximum and minimum; for k = 100, the plot does not have any extrema – all of this being consistent with the above analytical results.

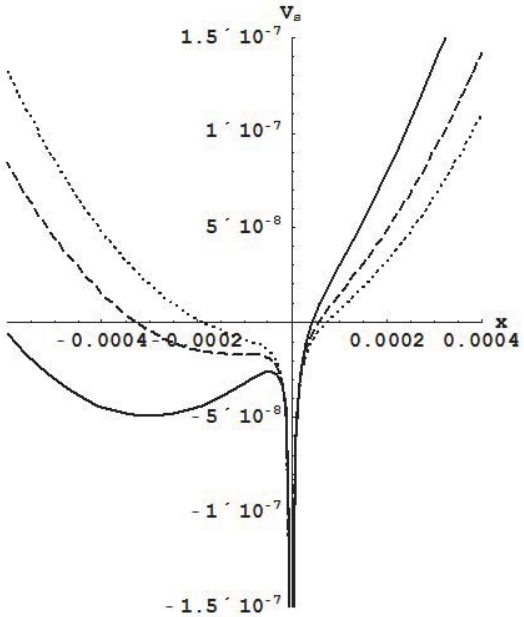

Fig. 2. The scaled potential energy V_s from Eq. (16) versus the coordinate x (cm) at the scaled magnetic field $b = 1.3 \times 10^6$ (corresponding to B = 5 Tesla) for the following three values of the scaled pseudomomentum: k = 400 corresponding to K = 1.25 a.u. (solid line), k = 206 corresponding to K = 0.64 a.u. (dashed line), k = 100 corresponding to K = 0.31 a.u. (dotted line).

Figure 3 presents the dependence of the location of the additional potential well x_1 (in cm) on the scaled magnetic field b and on the scaled pseudomomentum k in some ranges of these two parameters. It is seen that $|x_1|$ can reach "macroscopic" values, resulting in a GEDM of such state.

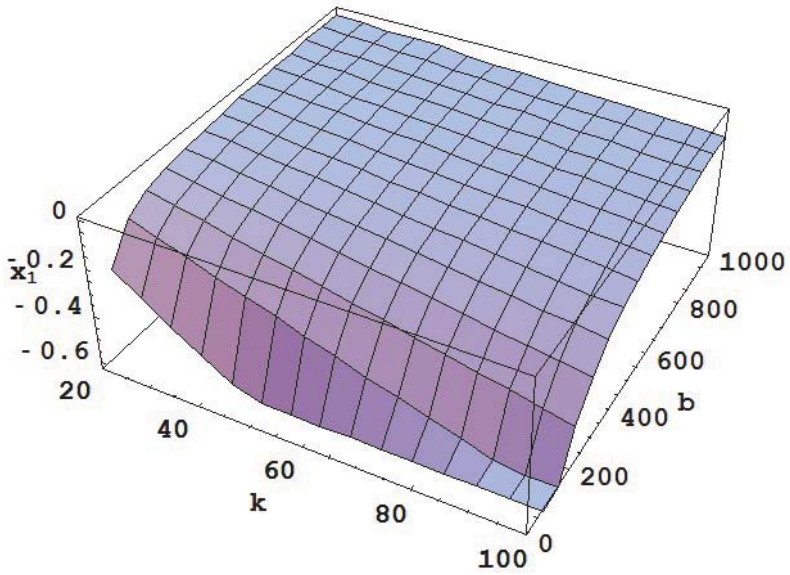

Fig. 3. Dependence of the location of the additional potential well x_1 (in cm) on the scaled magnetic field b and on the scaled pseudomomentum k.

Schmelcher and Cederbaum in their paper [7] gave only the following approximate formula for x_1 (converted below into our notations)

$$x_{1,CS} = -k/b + k/(k^3 - 2b). \tag{17}$$

As an example, Fig. 4 presents the ratio of the approximate root $x_{1,CS}$ from paper [7] to the exact root x_1 for the scaled pseudomomentum k = 20. It is seen, that for the given k, the relative error of the approximate formula (17) from paper [7] grows bigger as the scaled magnetic field b increases.

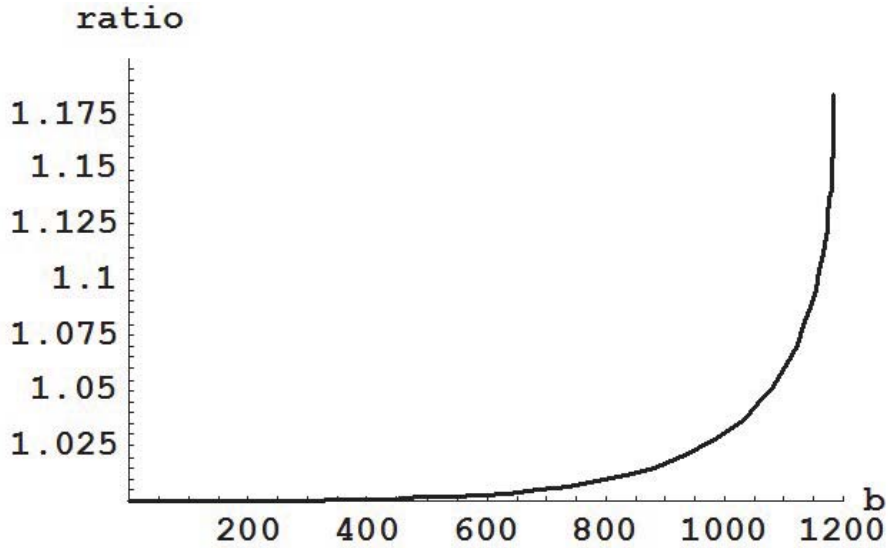

Fig. 4. The ratio of the approximate root $x_{1,CS}$ from paper [7] (reproduced in Eq. (17)) to the exact root x_1 for the scaled pseudomomentum k = 20.

Now let us discuss the corresponding profiles S(w) of hydrogen spectral lines in a magnetized plasma containing an electrostatic wave $\mathbf{F}\cos\omega t$ that propagates perpendicular to the magnetic field **B**. Here

$$w = \Delta\omega/\omega \tag{18}$$

is the scaled detuning from the unperturbed position of the spectral line. Figure 5 presents the orientation of the wave amplitude vector **F** with respect to the magnetic field **B**, the pseudomomentum **K**, and the giant dipole moment **d**, the latter corresponding to the state within the additional potential well located at $x_1 < 0$, where x_1 is given by Eq. (14).

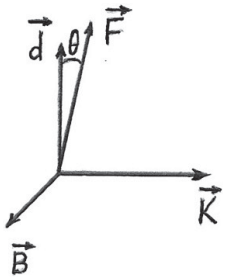

Fig. 5. The orientation of the amplitude vector F of an electrostatic wave in a magnetized plasma with respect to the magnetic field B, the pseudomomentum K, and the giant dipole moment d,, the latter corresponding to the state within the additional potential well located at $x_1 < 0$, where x_1 is given by Eq. (14).

Under the action of the field **F**cosωt, any atomic state possessing a permanent electric dipole moment **D** manifests in the spectral line profile as a series of Blokhinzew-type satellites at the distances qω (q = ±1, ±2, ±3, …) from the line center – see, e.g., paper [6] and Chapter 3 in book [8]. The actual number of observed satellites depends, first of all, on the so-called modulation parameter

$$\varepsilon = \mathbf{DF}/(\hbar\omega), \tag{19}$$

where **DF** stands for the scalar product (also known as the dot-product) of these two vectors. If $\varepsilon << 1$, then at best, practically only the satellites at ±ω might be observed (though not necessarily observed if the spectral line broadening by other mechanisms is relatively large). However, in the case of the GEDM states (the states within the additional potential well) there would be practically always $\varepsilon >> 1$. This situation corresponds to the multi-satellite regime where there would be numerous satellites of significant intensities: the satellites of the maximum intensity would be at $\Delta\omega \sim \pm\varepsilon\omega$. In this case, even if the spectral line broadening by other mechanisms is relatively large, one could observe the envelope of multiple satellites (rather than individual satellites), the maximum intensity of the envelope being at $\Delta\omega \sim \pm\varepsilon\omega$. More details and more precise formulas are presented in Chapter 3 of book [8].

Let us denote by g the share of hydrogen atoms that are in the GEDM states (the states within the additional potential well). We consider the case of a relatively weak electrostatic wave in a plasma, so that for hydrogen atoms that are not in the GEDM state, the corresponding modulation parameter from Eq. (19) is much smaller than unity. This means that for the share (1 – g) of hydrogen atoms, the would be satellites are extremely weak and practically do not affect spectral line profiles (e.g., for $\varepsilon \sim 10^{-3}$, the relative intensity of the "strongest" satellites would be $\sim 10^{-6}$). Then the total spectral line profile can be represented in the form

$$S(w) = (1 - g)\, S_0(w) + g S_1(w), \tag{20}$$

where

$$S_1(w) = \sum_{p=-\infty}^{\infty} J_p^2(\varepsilon_1)\, S_0(w - p), \qquad \varepsilon_1 = e|x_0|(F\cos\theta)/(\hbar\omega), \tag{21}$$

In Eq. (21), $J_p(\varepsilon_1)$ is the Bessel functions and e is the electron charge. As for the function $S_0(w)$ in Eqs. (20) and (21), it is the shape of the spectral line that would be at the absence of the electrostatic wave. It combines in the standard way the Doppler broadening, the Stark broadening by plasma ions and electrons, as well as the Zeeman effect – see, e.g., books [2, 9].

Below as an example, we consider the situation where the electrostatic wave in a plasma is the upper hybrid wave propagating perpendicular to the magnetic field **B**. Its well-known frequency is (see, e.g., book [10]):

$$\omega = (\omega_{ce}^2 + \omega_{pe}^2)^{1/2}. \quad (22)$$

Here

$$\omega_{ce} = eB/(m_e c) = 1.76x10^{11}B(\text{Tesla}), \quad (23)$$

is the electron cyclotron frequency (c being the speed of light) and

$$\omega_{pe} = (4\pi e^2 N_e/m_e)^{1/2} = 5.64x10^4[N_e(cm^{-3})]^{1/2} \quad (24)$$

is the plasma electron frequency, where N_e is the electron density.

For simplicity of formulas we consider the situation where $\omega_{ce} >> \omega_{pe}$, which is the case if

$$B >> B_{cr}(\text{Tesla}) = 3.21x10^{-7}\,[N_e(cm^{-3})]^{1/2}. \quad (25)$$

In this case, the upper hybrid wave frequency ω reduces practically to the electron cyclotron frequency ω_{ce}.

As an example, Fig. 6 shows the total profiles $S(\Delta\omega/\omega)$ of the Ly-beta line (solid curve) and the Ly-alpha line (dashed curve) for the case where g = 0.25, the magnetic field B = 5 Tesla, the plasma temperature T = 3 eV, the electron density $N_e = 3x10^{13}$ cm^{-3}, the pseudomomentum $K = 2.5x10^{-19}$ g cm/s = 1.25 at. units, and the projection of the amplitude vector of the upper hybrid wave on the giant dipole moment is F cosθ = 10 V/cm. In this case, $|x_0| = 3.0x10^{-4}$ cm = $5.7x10^4$ at. units and ε = 6. We note that B = 5 Tesla, T = 3 eV, and $N_e = 3x10^{13}$ cm^{-3} can correspond to the conditions of edge plasmas of tokamaks. The profiles $S(\Delta\omega/\omega)$ are area-normalized to unity.

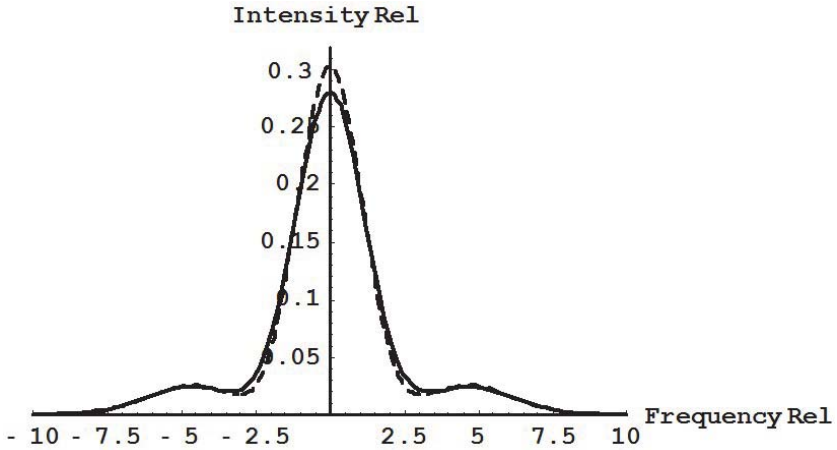

Fig. 6. Total profiles of the Ly-beta line (solid curve) and the Ly-alpha line (dashed curve) for the case where g = 0.25, the magnetic field B = 5 Tesla, the plasma temperature T = 3 eV, the pseudomomentum $K = 2.5x10^{-19}$ g cm/s = 1.25 at. units, and the projection of the amplitude vector of the upper hybrid wave on the giant electric dipole moment is F cosθ = 10 V/cm. The profiles $S(\Delta\omega/\omega)$ are area-normalized to unity.

It is seen that the *quasi-satellites*, i.e., the maxima of the envelope of multiple satellites are located at the same distance (in the frequency scale) from the line center for both spectral lines, this distance being significantly greater than the wave frequency.

Actually, *this is true for any two hydrogen lines*. This is the *distinctive feature* of the situation where a share of hydrogen atoms is in the GEDM states. Indeed, if there would not be such states and the wave amplitude would be large enough for having significant intensities of multiple Blokhinzew-type satellites, the maxima of the satellite envelopes would be at different distances from the line center for different hydrogen lines – see, e.g., book [8], Chapter 3.

In other words, if one would observe quasi-satellites (at the distance from the line center $\Delta\omega >> \omega$) in the experimental profile of just one hydrogen line, then both of the above interpretations would be possible. However, if one would observe the quasi-satellites at the same distance from the line center $\Delta\omega >> \omega$ in the experimental profiles of any two hydrogen lines, then the only possible interpretation would be as follows. First, it would be the manifestation

of the presence of the GEDM states of hydrogen atoms. Second, this would constitute a supersensitive method for spectroscopic diagnostics of electrostatic waves in magnetized plasmas – namely, the waves of the amplitude as low as ~ 10 V/cm or even lower.

3. CONCLUSIONS

We considered how the GEDM states manifest in the profiles of hydrogen spectral lines in the presence of a quasimonochromatic electrostatic wave of a frequency ω in a plasma. We demonstrated that in this situation, hydrogen spectral lines can exhibit quasi-satellites, which are the envelopes of Blochinzew-type satellites.

We showed that the *distinctive feature* of such quasi-satellites is that their peak intensity is located at the same distance from the line center (in the frequency scale) for all hydrogen spectral lines, the distance being significantly greater than the wave frequency ω. At the absence of the GEDM (and for relatively strong electrostatic waves), the maxima of the satellite envelopes would be at different distances from the line center for different hydrogen lines.

We demonstrated that this effect would constitute a *supersensitive diagnostic method*. It would allow measuring the amplitude of electrostatic waves in plasmas down to ~ 10 V/cm or even lower.

Author Contribution Statement. All authors contributed equally to the paper.

References

1. H.-J. Kunze, *Introduction to Plasma Spectroscopy* (Springer, Berlin) 2009.
2. E. Oks, *Diagnostics of Laboratory and Astrophysical Plasmas Using Spectral Lines of One-, Two-, and Three-Electron Systems* (World Scientific, New Jersey) 2017.
3. P. Schmelcher and L.S. Cederbaum, Phys Rev. Letters **74** (1995) 662.
4. P. Schmelcher and L.S. Cederbaum, Phys Rev. A **47** (1993) 2634.
5. M. Vincke and D. Baye, J. Phys. B: At. Mol. Opt. Phys. **21** (1988) 2407.
6. D.I. Blochinzew, Phys. Z. Sov. Union **4** (1933) 501.
7. P. Schmelcher and L.S. Cederbaum, Chem. Phys. Letters **208** (1993) 548.
8. E. Oks, *Plasma Spectroscopy: The Influence of Microwave and Laser Fields* (Springer, Berlin) 1995.
9. H.R. Griem, *Principles of Plasma Spectroscopy* (Cambridge University Press, Cambridge) 1977.
10. D.G. Swanson, *Plasma Waves* (Academic Press, Cambridge, MA, USA) 2012.